Covalent Crosslinked Assembly of Tubular Ceramic-based Multilayer Nanofiltration Membranes for Dye Desalination

Lu Wang, Naixin Wang, Guojun Zhang, and Shulan Ji
Center for Membrane Technology, College of Environmental and Energy Engineering, Beijing University of Technology, Beijing 100124, P.R. China

DOI 10.1002/aic.14093
Published online April 25, 2013 in Wiley Online Library (wileyonlinelibrary.com)

A tubular ceramic-based multilayer composite nanofiltration membrane has been developed for dye desalination. Poly(acrylic acid)(PAA)/poly(vinyl alcohol)(PVA)/glutaraldehyde(GA) was dynamically assembled on to the inner surfaces of tubular ceramic microporous substrates which had been pretreated using dynasylan ameo silane coupling agents. Subsequently, the composite membranes were thermally crosslinked to form covalent ester bonds. Experimental results proved that the composite membrane had good nanofiltration performance for dye desalination. The (GA/PVA/PAA)$_3$/ceramic multilayer membrane shows over 96% retention of Congo red and less than 3% NaCl retention using a permeate flux of about 25 L/(m^2·h). An investigation of membrane performance as a function of operating conditions suggested that the covalent crosslinking multilayer membrane possessed much higher stability compared to other, electrostatically assembled, multilayer membranes. © 2013 American Institute of Chemical Engineers *AIChE J*, 59: 3834–3842, 2013
Keywords: organic–inorganic composite membrane, tubular, covalent reaction, nanofiltration, layer-by-layer

Introduction

Currently, dyes are widely used in many fields such as the textile, article and food industries.[1,2] Generally, dyes are produced by chemical synthesis, using methods that involve much salt, small molecular weight intermediates and residual compounds. Consequently, the dyes must be purified before commercial use. Conventionally, the dye is precipitated from an aqueous solution using salt.[3,4] This method can introduce a lot of salt to the dye, affecting its stability, color and purity. To improve the quality, dye desalination is very important. Nanofiltration (NF) is usually used for the purification of a variety of dyes from salt solutions because of the low-energy requirement, high-permeation flux and relatively low investment and maintenance costs.[5,6] At present, most NF membranes are prepared by an interfacial polymerization method.[7,8] In recent years, the layer-by-layer (LbL) technique has been widely used to prepare film materials with precise control on the nanoscale of size, composition and morphology.[9,10] In particular, LbL-assembled membranes show great potential for separation applications, such as pervaporation,[11–14] gas separation,[15] nanofiltration,[16,17] reverse osmosis[18] and forward osmosis.[19,20] However, most research has been focused on the electrostatic attraction between oppositely charged polymers as the driving-force for assembly of the membranes.[21–23] The stability of these electrostatically assembled membranes is usually weak. Polyelectrolyte multilayer can become unstable and breaking-up in high-salt concentrations and extreme pH values.[24,25] This seriously limits practical separation applications so it is very important to improve the structural stability of such multilayers. By comparison, covalent assembly and post-crosslinking might readily yield more stable structures. In fact, some researchers have assembled multilayers using direct covalent LbL. For instance, Lynn and coworkers reported a layer-by-layer approach to the assembly of covalently-crosslinked ultrathin films that makes use of fast and efficient "click"-type interfacial reactions.[26] Caruso and coworkers demonstrated that the stable single-component poly(acrylic acid) (PAA) films can be obtained using click chemistry under mild aqueous conditions.[27] Our group has previously reported the covalent assembly of a polyethyleneimine (PEI)/glutaraldehyde multilayer membrane for pervaporation separation applications.[28] The covalently assembled multilayer membranes showed much higher stabilities compared with those prepared by electrostatically LbL assembly methods, and offer many opportunities for practical applications.

More recently, attempts to combine the advantages of both polymeric and ceramic membranes have attracted significant attention.[13,29] For example, Jin et al. have successfully prepared an organic–inorganic composite membrane by means of electrostatic self-assembly of polyelectrolytes on silica sol–gel modified macroporous ceramic supports.[30] We have reported the use of a hollow fiber ceramic-based PAA/PEI multilayer composite membrane for pervaporation dehydration of alcohol–water mixtures.[31] Compared with more conventional pervaporation membranes, studies of organic–inorganic composite nanofiltration membranes are relatively few in number. Actually, NF membranes usually operate at much higher pressure (from 3 to 14 bar) than pervaporation membranes.[32] The development of an organic–inorganic composite membrane might be also a good choice for

Correspondence concerning this article should be addressed to G. Zhang at zhanggi@bjut.edu.cn.

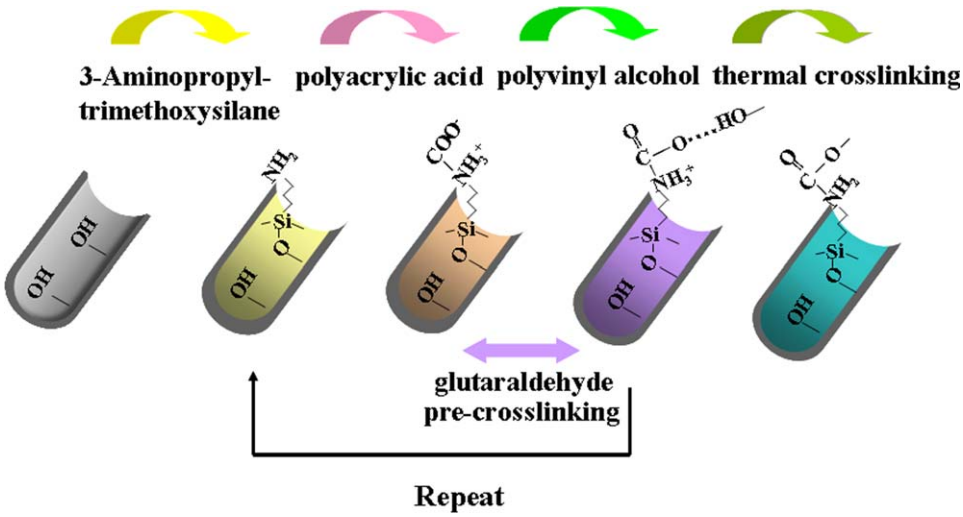

Figure 1. Schematic illustration of the preparation of covalent crosslinked multilayer on an inner surface of tubular ceramic substrate membrane.

[Color figure can be viewed in the online issue, which is available at wileyonlinelibrary.com.]

nanofiltration because the ceramic porous substrates provide mechanical stability, while the polymeric layer is responsible for selective separation. In addition to the membrane material, the selection of the membrane support is also crucial; as this decides in which way the membranes should be packaged. For instance, tubular ceramic membranes have proved to be more effective than flat-sheet arrangements, because of their higher packing density leading to a more compact product. Recently, considerable interest has been shown in hollow fiber ceramic membranes.[33–35] However, their brittleness and high cost have limited their applications. By comparison, tubular ceramic membranes present the most mature and most widely used module form. In addition to the advantages of mechanical strength and low price, tubular membranes are suitable for handling viscous liquids with high levels of suspended solids. They can also be chemically or mechanically cleaned. In particular, if a dense selective layer is formed on the inner surface of tubular ceramic supports, the organic separation layer can be easily protected. Moreover, this type of module can provide good distribution of feed solution because the tubular membrane itself can be used as the liquid distributor.[36] In summary, inner skin tubular ceramic-based membranes might be a good alternative to the inorganic–organic composite NF membrane.

In this article, ceramic-based nanofiltration was attempted using a covalent crosslinked assembly of hydrophilic polymers on the inner surface of tubular porous ultrafiltration modules. As shown in Figure 1, the stable siloxane bonds (—Si—O-ceramic) were formed by pretreating the ceramic supporting porous membrane with dynasylan ameo (DA) silane coupling agents.[37] Subsequently, the poly(acrylic acid)/poly(vinyl alcohol) multilayer can be successfully deposited on to the inner surfaces of the tubular ceramic porous substrates using a dynamic LbL assembly technique. Glutaraldehyde was used to pre-crosslink the hydrophilic multilayer. Then, the multilayer membranes were thermally crosslinked via dehydration between the carboxylic acid and hydroxyl groups.[38] Micrographs of the organic–inorganic composite membranes were recorded using a scanning electron microscope (SEM). Finally, the nanofiltration performance of the composite membranes was measured by studying the separation of dye/salt mixtures.

Experimental

Materials

All chemicals were used as received. Poly(acrylic acid) (PAA, Mw 4,000,000) and 3-Aminopropyl-trimethoxysilane (dynasylan ameo silane coupling agent, Mw 179.29) were purchased from Aldrich. Glutaraldehyde(GA), poly(vinyl alcohol) (PVA, Mw 2000,16,000 and 80,000), congo red, methylene blue, acid fuchsin and methyl orange were provided by the Beijing Chemical factory. The tubular ceramic substrate membranes were purchased from Foshan Science and Technology factory; these had average pore sizes of 100–200 nm. The porous Al_2O_3 tubes have a wall thickness of 2 mm (internal dia. = 8 mm; outside dia. = 12 mm).

Preparation of tubular ceramic-based nanofiltraion membrane

Pretreatment of the ceramic tube was performed using immersion of a mixture of ethanol (EtOH) solution ($EtOH:H_2O = 95:5$) and 2 g/L DA silane coupling agent at room temperature for 2 h, followed by rinsing with deionized water and drying in air at 110°C for 2 h in a vacuum oven. 0.05 wt % PAA, 4 wt % PVA and 0.75 wt % GA solutions were prepared. A newly developed dynamic negative LbL technique was used to construct the multilayers on to the pretreated ceramic membrane.[39,40] As shown in Figure 2a, the PAA solution was passed through the inner channel of the tubular membrane and then recycled using an external peristaltic pump. A negative pressure of −0.09 MPa was created on the outer surface by a water circulating pump (SHB-3A, Zhengzhou Greatwall Scientific Industrial and Trading Co., Ltd.). After passage of the PAA, PVA solution was assembled on to the inner surface of the ceramic support in the same way (Figure 2b). GA solution was then used to pre-crosslink the PVA layer by passing it through the inner channel of the tubular membrane at a pressure of 0.09 MPa (Figure 2c). The (GA/PVA/PAA)n multilayer membrane was obtained by repeating the above assembly steps n times. The assembly time for each PAA, PVA and GA step was 15 min. After assembly, the composite membrane was dried at 75°C for about 60 min then the subsequent polymeric

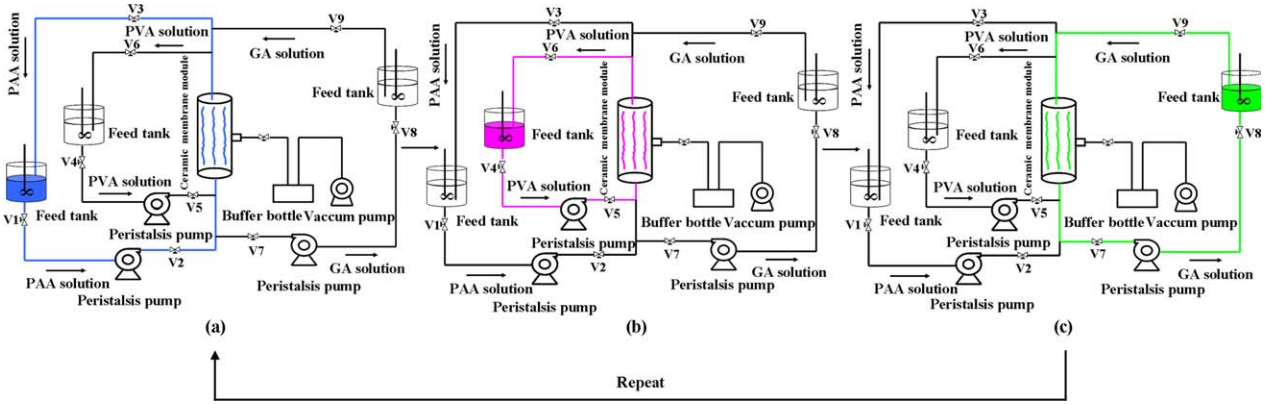

Figure 2. Experimental apparatus for the preparation of covalent crosslinked multilayer on an inner surface of tubular ceramic substrate membrane by a dynamic pressure-driven LbL assembly.

[Color figure can be viewed in the online issue, which is available at wileyonlinelibrary.com.]

multilayer was thermally crosslinked in a vacuum oven at 150°C for 2 h.

Nanofiltration experiments

The tubular module for the nanofiltration test consisted of one ceramic membrane, with an effective length of 9 cm and effective area of 26 cm^2. Congo red, methylene blue, acid fuchsin and methyl orange were used as model dyes. The experiments were carried out at a pressure of 0.6 MPa produced by a plunger pump. Fluxes were determined by measuring the volume of liquid collected over a measured time under steady-state conditions. The permeate flux (J) was calculated as follows

$$J = \frac{V}{t \cdot A}$$

where V is the permeate volume (l), t stands for the time (hours), and A denotes the effective membrane surface area (m^2).

The rejection was defined by

$$R = \frac{C_k - C_p}{C_k}$$

where C_k and C_p denote the dye and salt concentration (mg/L) in the retentate and permeate, respectively. The dye concentrations were measured using an ultraviolet-visible spectrophotometer (UV-2550, Japan) at the maximal absorption wavelength of each organic anionic dye. The salt concentration was obtained through the measurement of the conductivity of the aqueous solution using a conductivity meter (DDS-12A, RiDao Instruments, Shanghai).

Characterization

The attenuated total reflectance FTIR spectra (Vertex-70, Bruker, Germany) were used to confirm the formation of covalent bonds. Measurements were carried out at room temperature. An electrokinetic analyzer (SurPASS, Anton Paar) was used to determine the zeta potential variations of membrane surface. In the measurement process, the concentration of the electrolyte maintained at about 0.83 mmol/L, with an operating pressure of 0.03 MPa. The surface and cross-sectional morphologies of the tubular ceramic membranes and the thicknesses of the organic separation layers were characterized by scanning electron microscopy (SEM) (Hitachi S-4300, Japan).

Results and Discussion

Zeta potential and FTIR analyses

The zeta potential analyses were used for detecting the presence of multilayers on to the inner surfaces of the tubular ceramic substrate. Figure 3 shows the variation of the inner surface zeta potential with layer number. It was noted that the ceramic surface had a negative potential of −237.92 mV. The surface potential was reversed to a positive value after pretreatment by the silane coupling agents, which are positively charged because of the amino groups. After assembling one PAA layer, the charge on the inner surface was shifted to a negative value. Because the charged carboxylate groups of PAA can react with the hydroxyl groups of PVA, the overall negative charge decreased after reaction.

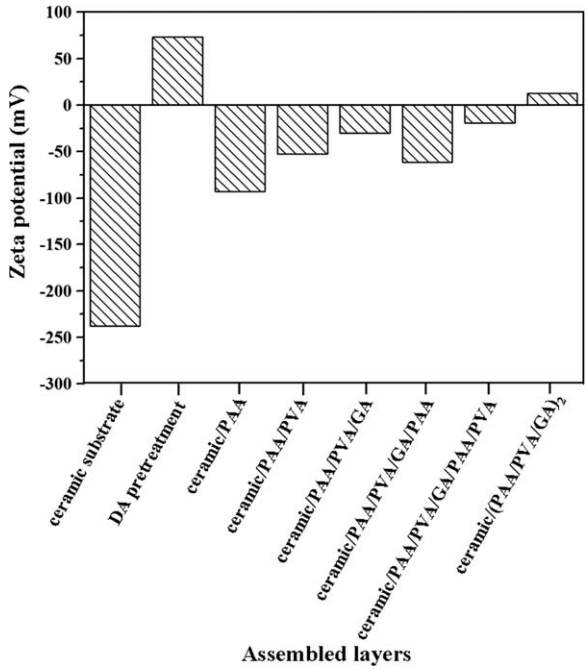

Figure 3. Variations of inner surface zeta potential with different assembled layers.

Preparative conditions: 15 min filtration time, 0.05 wt % PAA aqueous solution, 4 wt % PVA (MW 80000) aqueous solution, 0.75 wt % GA aqueous solution, dynamic negative pressure −0.09 MPa.

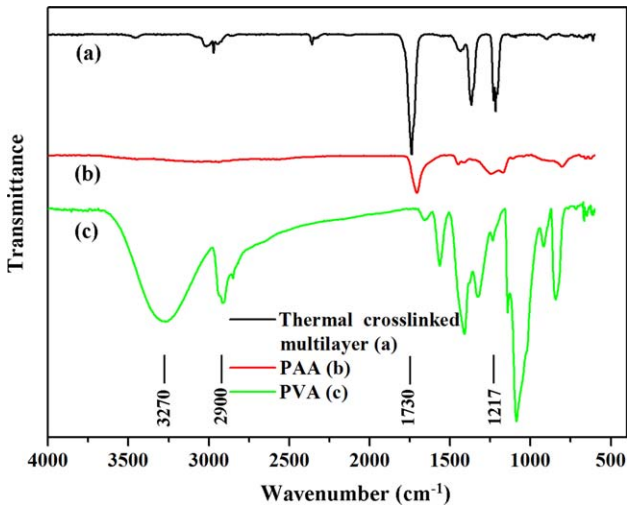

Figure 4. FTIR spectra of (a) thermal crosslinked multilayer, (b) PAA, and (c) PVA.

Preparative conditions: 3 trilayers, 15 min filtration time, 0.05 wt % PAA aqueous solution, 4 wt % PVA (Mw 80000) aqueous solution, 0.75 wt % GA aqueous solution, dynamic negative pressure −0.09 MPa, thermal crosslinking time 2 h, thermal crosslinking temperature 150°C. [Color figure can be viewed in the online issue, which is available at wileyonlinelibrary.com.]

After crosslinking with GA, the negative charge can decrease further.

To further demonstrate the formation of chemical bond between PAA and PVA, the FTIR spectra were investigated. The FTIR spectra of PVA, PAA and the thermally crosslinked PVA/PAA composite membrane are shown in Figure 4. In the spectrum of PVA, the broad band at 3100– 3500 cm^{-1} is attributed to the —OH group. A peak at 1730 cm^{-1} was observed in the spectrum of PAA, which corresponds to the —C═O vibration of the carboxylic acid group in PAA. In the spectrum of the crosslinked composite membrane, the —OH group at 3100–3500 cm^{-1} has disappeared while the —C═O group, which can be identified from the ester group (—COO—) absorption at 1730 cm^{-1}, increased in intensity. These changes suggested the formation of ester bonds due to the dehydration reaction between carboxylate groups (PAA) and hydroxyl groups (PVA).

Morphology of the membranes

The inner surface and cross-sectional morphologies of the ceramic-based multilayer membranes were characterized with SEM. As shown in Figure 5a, many nanoscale pores were observed on the inner surface of ceramic substrate. After assembly of one PAA/PVA/GA layer, some defects were still observed on the surface of the membrane (Figure 5b). After assembly of between three and five PAA/PVA/GA layers, a dense and defect-free selective layer was formed on the substrate membrane (Figure 5c and d). The surface looks very smooth. Comparing Figure 5e with 5h, we can see clearly that organic separation layers have been successfully coated on to the inner surface of the ceramic substrate. Moreover, the thickness of separation layers increased gradually with the increase in the number of layers (Figure 5f, g and h). As can be seen from Figure 5h, the thickness of the organic separation layers was about 10 μm for five PAA/PVA/GA layers. This is clearly a facile way to control the thickness of the selective layer using this dynamic assembly method.

Effects of PVA molecular weight and layer numbers

The inner skin tubular ceramic-based nanofiltration membrane, prepared as described above, was subsequently used to study dye retention. The effects of the PVA molecular weight on the nanofiltration performance were investigated, with the results shown in Figure 6. For example, the retention increased from 51.54% to 97.11% while the flux significantly decreased from 55.31 L/(m^2·h) to 20.15 L/(m^2·h) for a change of PVA molecular weight from 2000 to 80,000. Clearly, the higher molecular weight PVA is beneficial for the formation of denser separation layers and consequently a higher retention NF membrane. Therefore, the PVA with a molecular weight of 80,000 was adopted for subsequent study.

Usually, the number of layers plays a very important role in membrane performance. The retention of congo red with different numbers of trilayers is shown in Figure 7. It was observed that, with increasing numbers of PAA/PVA/GA layers, the rejection increased while the flux decreased. For example, the retention of congo red was 92.2% with one PAA/PVA/GA trilayer deposited, but the rejection rapidly reached 97.3 and 99% for three and five PAA/PVA/GA trilayers, respectively. Simultaneously, the total flux decreased from about 51.15 L/(m^2·h) to 25.24 L/(m^2·h) and 8.2 L/(m^2·h). This was because that the increase in the number of polymer pairs usually resulted in the formation of much denser and more compact separation layers. The performance can easily be tuned by the assembly of membranes with different numbers of polymer pairs. Considering the necessary compromise between retention and permeation capabilities, three PAA/PVA/GA trilayers was selected for subsequent experiments.

The membrane was also evaluated using different dye solutions. As shown in Figure 8, the molecular weights of the three organic dyes involved in the tests were very different. The composite membranes have good rejection when they are used to separate acid fuchsin, congo red and methylene blue. For methylene blue in particular, the rejection reached 99.8% and the flux was 18.35 L/(m^2·h). It is worth noting that a low-molecular-weight dye, such as methyl orange, gave a rejection value of about 40% with a flux of 39.8 L/(m^2·h). This is accordance with the study by Katarzyna et al. They found that dyes with molecular weight less than about 600 show poor rejection.[41]

Dye desalination of tubular ceramic-based NF membrane

It is well-known that the presence of salts in the dye solutions will affect the rejection and the permeation flux. Dye desalination is a very important process for dye production so the effects of salt on the flux and dye retention were investigated. It can be seen from Figure 9 that, as the feed NaCl concentration increased from 1000 to 5000 mg/L, the dye retention rate decreased slightly, from about 97.6% to 96.3%, while the flux clearly increased, from 25.1 to 29.6 L/(m^2·h). This is mainly attributed to the salt ions which couple with the charged dye molecules. The salt can be dispersed uniformly in aqueous solution, dispersing the dye molecules more uniformly.[42] Therefore, any concentration polarization and membrane fouling will be reduced. As a result, there is an increase of flux with increasing feed salt concentration. It was also noted that the retention rate of NaCl always remained below 3%. This suggested that most

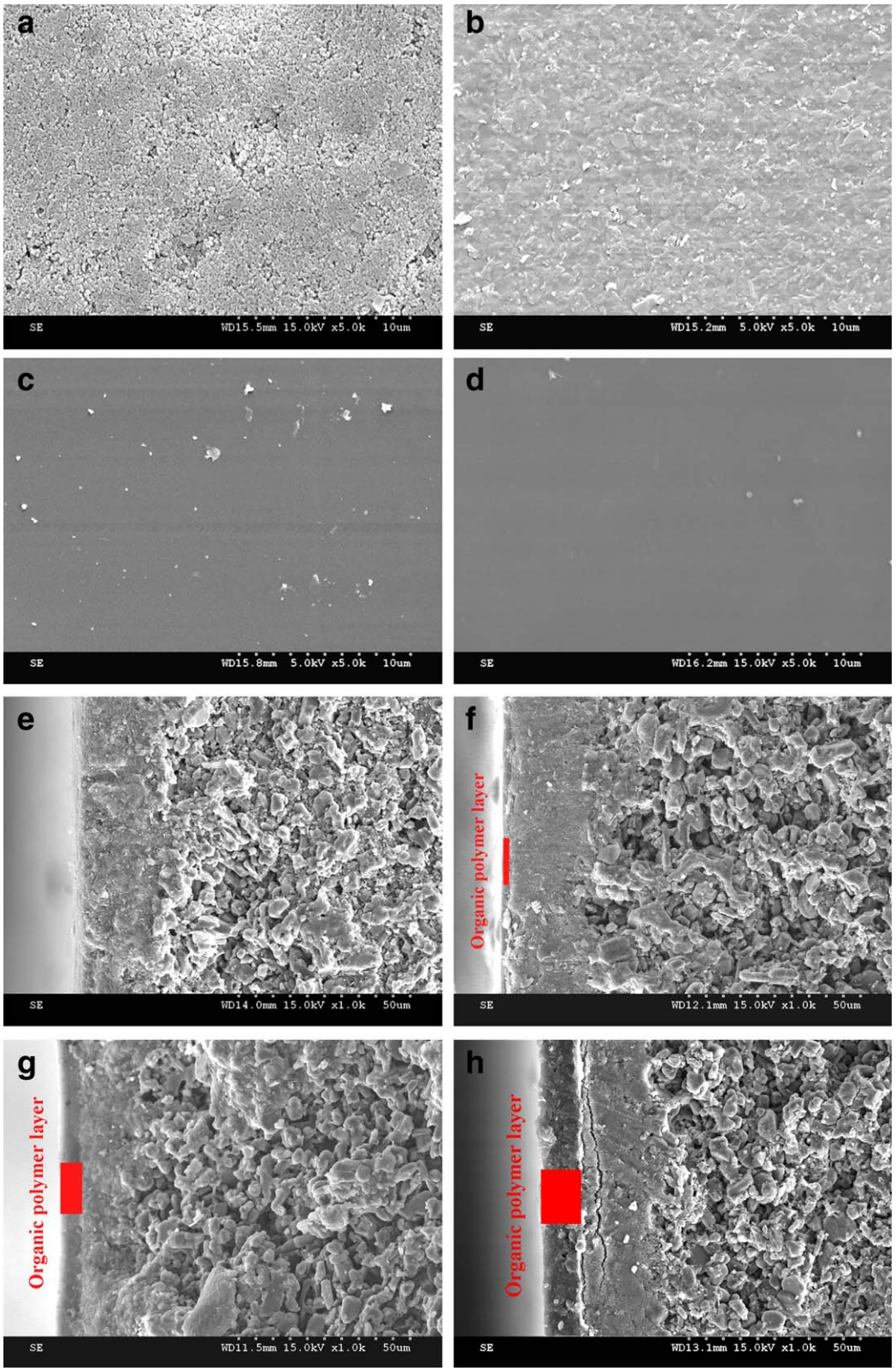

Figure 5. SEM images of the tubular membranes.

(a) Inner surface of the ceramic substrate (5.0 k×), (b) inner surface after assembling one PAA/PVA/GA trilayer (5.0 k×), (c) inner surface after assembling three PAA/PVA/GA trilayers (5.0 k×), (d) inner surface after assembling five PAA/PVA/GA trilayers (5.0 k×)l (e) cross section of tubular ceramic substrate(1.0 k×)l (f) cross section of tubular ceramic-based after assembling one PAA/PVA/GA trilayer (1.0 k×), (g) cross section after assembling three PAA/PVA/GA trilayers (1.0 k×), and (h) cross section after assembling five PAA/PVA/GA trilayers (1.0 k×). Preparative conditions: 15 min filtration time, 0.05 wt % PAA aqueous solution, 4 wt % PVA (Mw 80000) aqueous solution, 0.75 wt % GA aqueous solution, dynamic negative pressure −0.09 MPa, thermal crosslinking time 2 h, thermal crosslinking temperature 150°C. [Color figure can be viewed in the online issue, which is available at wileyonlinelibrary.com.]

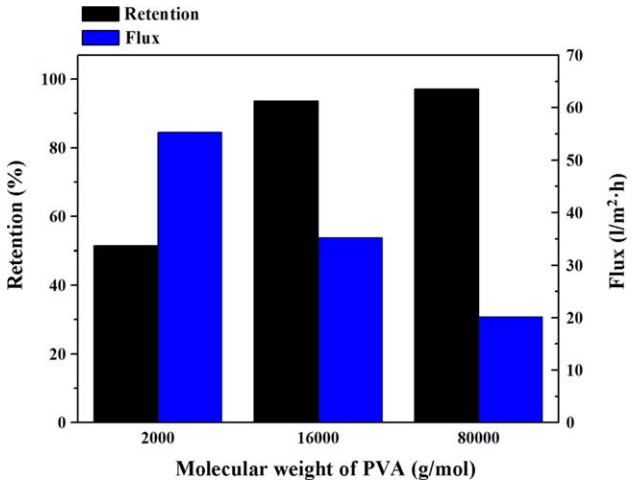

Figure 6. Effects of PVA molecular weight on nanofiltration performance.

Preparative conditions: 3 trilayers, 15 min filtration time, 0.05 wt % PAA aqueous solution, 4 wt % PVA aqueous solution, 0.75 wt % GA aqueous solution, dynamic negative pressure −0.09 MPa, thermal crosslinking time 2 h, thermal crosslinking temperature 150°C; nanotiltration conditions: 0.6 MPa, 25°C, 100 mg/L Congo red. [Color figure can be viewed in the online issue, which is available at wileyonlinelibrary.com.]

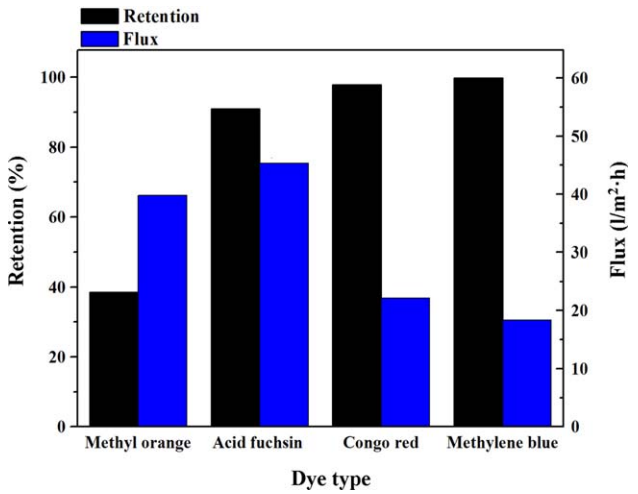

Figure 8. Nanofiltration performance for different dye solutions.

Preparative conditions: 3 tri-layers, 15 min filtration time, 0.05 wt % PAA aqueous solution, 4 wt % PVA(Mw 80000) aqueous solution, 0.75 wt % GA aqueous solution, dynamic negative pressure −0.09 MPa, thermal crosslinking time 2 h, thermal crosslinking temperature 150°C; nanotiltration conditions: 0.6 MPa, 25°C, 100 mg/L dye solution. [Color figure can be viewed in the online issue, which is available at wileyonlinelibrary.com.]

of the salt ions could pass easily through the multilayer membrane even when the dye molecules were efficiently retained, a property which is very beneficial for dye desalination.

Figure 10 shows the changes of rejection and flux with dye concentration. It is apparent that with increasing concentration of congo red, the flux decreased while the retention rate of the congo red dye remained constant. For example, as the feed dye concentration increased from 100 to 300 mg/L, the water permeate flux was steadily reduced, from about 25.1 to 19.8 L/m^2 h, while the rejection was maintained at about 97%. The rejection of NaCl was less than 2%. A possible reason for this is that the increase of dye concentration leads to an increase of dye adsorption on the membrane surface, which leads to serious concentration polarization, an increase of the resistance to water permeation and consequently a decline in the permeate flux.[43]

The effects of operating pressure on the nanofiltration separation of dye/salt mixture were also investigated. As shown in Figure 11, with increasing pressure, the permeate flux of the dye solution increased while the rejection of dye remained relatively stable. The permeate flux of the dye solution was as low as 5.1 L/(m^2·h) at 0.2 MPa, but reached

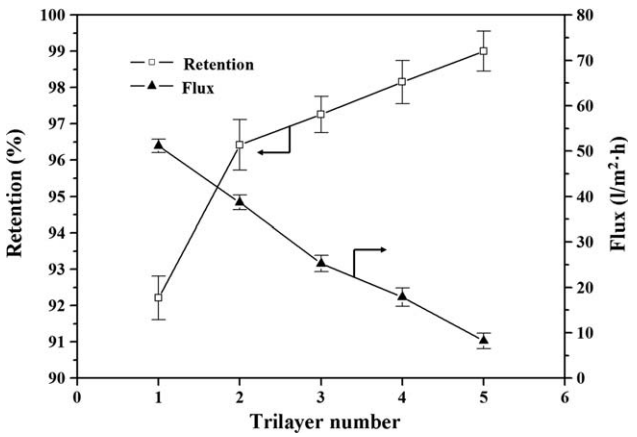

Figure 7. Effects of trilayer numbers on nanofiltration performance.

Preparative conditions: 15 min filtration time, 0.05 wt % PAA aqueous solution, 4 wt % PVA (Mw 80000) aqueous solution, 0.75% GA aqueous solution, dynamic negative pressure −0.09 MPa, thermal crosslinking time 2 h, thermal crosslinking temperature 150°C; nanotiltration conditions: 0.6 MPa, 25 °C, 100 mg/L congo red.

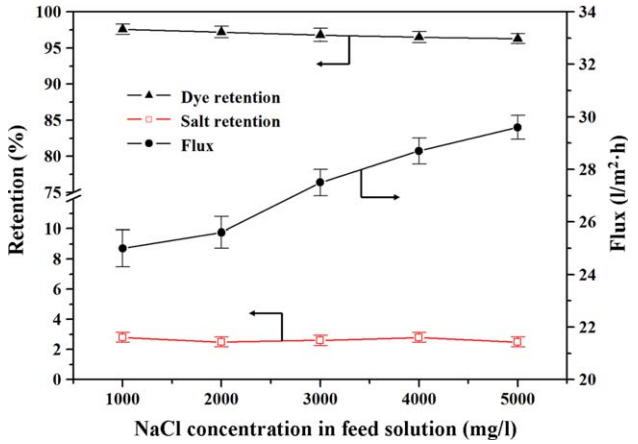

Figure 9. Effects of feed NaCl concentration on nanofiltration performance.

Preparative condition: 3 trilayers, 15 min filtration time, 0.05 wt % PAA aqueous solution, 4 wt % PVA(Mw 80000) aqueous solution, 0.75 wt % GA aqueous solution, dynamic negative pressure −0.09 MPa, thermal crosslinking time 2 h, thermal crosslinking temperature 150°C; nanofiltration condition: 0.6 MPa, 25°C, 100 mg/L congo red. [Color figure can be viewed in the online issue, which is available at wileyonlinelibrary.com.]

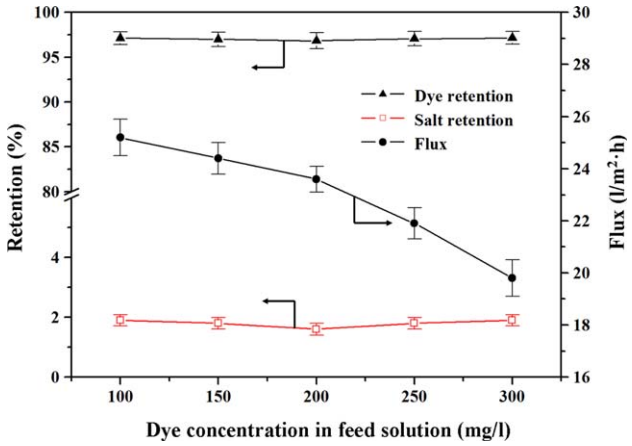

Figure 10. Effects of feed dye concentration on nanofiltration performance.

Preparative condition: 3 trilayers, 15 min filtration time, 0.05 wt % PAA aqueous solution, 4 wt % PVA(Mw 80000) aqueous solution, 0.75 wt % GA aqueous solution, dynamic negative pressure −0.09 MPa, thermal crosslinking time 2 h, thermal crosslinking temperature 150°C; nanotiltration condition: 0.6 MPa, 25°C, 1000 mg/L NaCl. [Color figure can be viewed in the online issue, which is available at wileyonlinelibrary.com.]

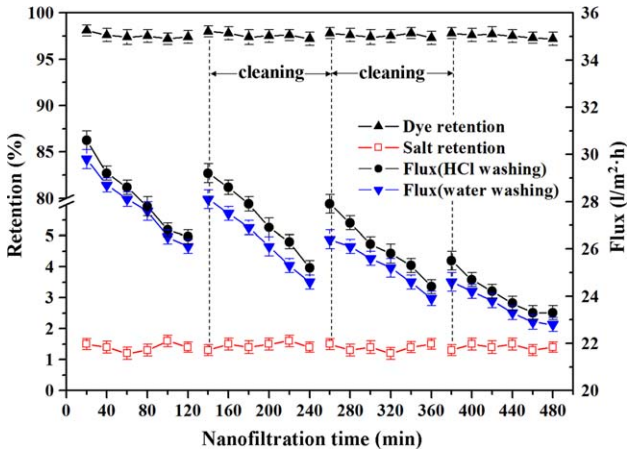

Figure 12. Variations of membrane performance with nanofiltration time.

Preparative conditions: 3 trilayers, 15 min filtration time, 0.05 wt % PAA aqueous solution, 4 wt % PVA (Mw 80000) aqueous solution, 0.75 wt % GA aqueous solution, dynamic negative pressure −0.09 MPa, thermal crosslinking time 2 h, thermal crosslinking temperature 150°C; nanotiltration conditions: 0.6 MPa, 25°C, 100 mg/L congo red, 1000 mg/L NaCl. [Color figure can be viewed in the online issue, which is available at wileyonlinelibrary.com.]

24.2 L/(m^2·h) at 0.6 MPa. The rejection for NaCl was stable and remained at about 1.3%. The aforementioned results suggest that the nanofiltration separation capability for dye molecules and NaCl using the covalent crosslinking multilayer membrane was very stable, independent of operation conditions.

Membrane fouling and cleaning

Membrane fouling is an inevitable phenomenon which has great influence on the membrane operation and a preliminary study was carried out to try to understand this. Figure 12 shows the variation of permeate flux and rejection for dye solutions over an operating period of 8 h. During operation, the membrane was washed with pure water every 2 h. As shown in Figure 12, the flux decreased with time during each run. This is because of the increase of adsorption of the dye on to the membrane surface as the experiment proceeded. However, the flux partly recovered when the membrane was washed with pure water. Since acid cleaning is the most frequently used membrane cleaning method,[44,45] chemical cleaning using 0.24% HCl solution was also carried out every 2 h. Compared to water washing, the flux recovered more after HCl washing. Clearly, some dye molecules deposited on membrane surface can be dissolved in acid solution and rinsed off, which reduces the resistance to water permeation. In addition, whether the membrane was washed with pure water or HCl, the rejection of dye and NaCl were almost unchanged, remaining at 97 and 1.4%, respectively. These results suggest that the multilayer membrane is very stable even in the presence of acids and salts. As a control, it has previously been demonstrated that the electrostatically assembled multilayer membranes could be partially decomposed, particularly in salt and acid solutions.[46,47] Therefore, it is likely that this covalently crosslinked multilayer membrane, with much higher stability, offers considerable opportunity for practical applications in the dye desalination field, even for the subsequent cleaning process.

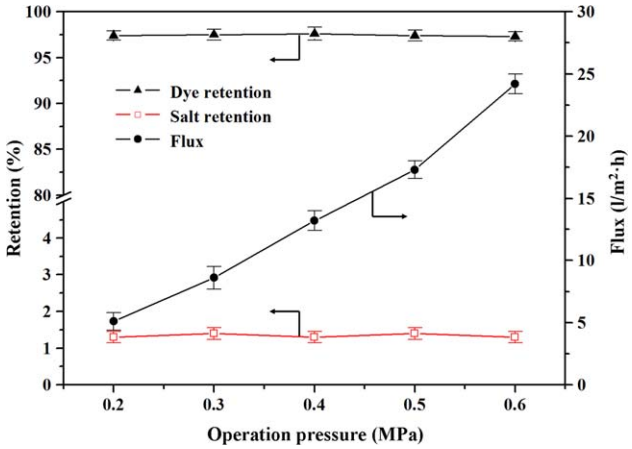

Figure 11. Effect of operating pressure on nanofiltration performance.

Preparative conditions: 3 trilayers, 15 min filtration time, 0.05 wt % PAA aqueous solution, 4 wt % PVA (Mw 80000) aqueous solution, 0.75 wt % GA aqueous solution, dynamic negative pressure −0.09 MPa, thermal crosslinking time 2 h, thermal crosslinking temperature 150°C; nanotiltration conditions: 25°C, 100 mg/L congo red, 1000 mg/L NaCl. [Color figure can be viewed in the online issue, which is available at wileyonlinelibrary.com.]

Conclusions

In summary, an inner skin tubular ceramic-based multilayer nanofiltration membrane was successfully prepared using a dynamic LbL assembly and thermal covalent crosslinking technique. The process of assembly was characterized by FTIR, SEM and an electrokinetic analyzer. The inner skin tubular ceramic-based multilayer nanofiltration membrane shows excellent performance for the separation of

dye and salt. In the case of the NF separation of 100 mg/L congo red and 1000 mg/L NaCl, the membrane had over 96% dye retention and less than 3.0% salt retention with a permeate flux of 25 L/(m^2·h), respectively. It was also noted that the nanofiltration performance of this organic–inorganic multilayer membrane could be easily tuned by changing the number of trilayers and the molecular weight of the PVA. One of the most important advantages is that the covalently crosslinked multilayers are more stable than those prepared by the electrostatic LbL approach even in salt and acid solutions. The rejection of dye and NaCl can remain almost unchanged after HCl washing. Therefore, it is believed that this organic–inorganic multilayer membrane has great potential for separation applications.

Acknowledgments

This work was financially supported by the National High Technology Research and Development Program of China (No. 2012AA03A607), Natural Science Foundation of Beijing (Nos. 8122010, 8102008), the National Basic Research Program of China (No.2009CB623404), Program for New Century Excellent Talents in University, Ministry of Education, China (No. NCET-12-0604), and Fok Ying Tung Education Foundation (No.131068).

Literature Cited

1. Bardajee G, Li A, Haley J, Winnik M. The synthesis and spectroscopic properties of novel, functional fluorescent naphthalimide dyes. *Dyes Pigments* 2008;79:24–32.
2. Klochko O, Fedyunyayeva I, Khabuseva S, Semenova O, Terpetschnig E, Patsenker L. Benzodipyrrolenine-based biscyanine dyes: Synthesis, molecular structure and spectroscopic characterization. *Dyes Pigments*. 2010;85:7–15.
3. Huang J, Zhang K. The high flux poly(m-phenylene isophthalamide) nanofiltration membrane for dye purification and desalination. *Desalination.* 2011;282:19–26.
4. He Y, Li G, Wang H, Zhao J, Su H, Huang Q. Effect of operating conditions on separation performance of reactive dye solution with membrane process. *J Membr Sci*. 2008;321:183–189.
5. Han R, Zhang S, Xing D, Jian X. Desalination of dye utilizing copoly(phthalazinone biphenyl ether sulfone) ultrafiltration membrane with low molecular weight cut-off. *J Membr Sci*. 2010;358:1–6.
6. Elazhar F, Tahaikt M, Achatei A, Elmidaoui F, Taky M, Hannouni F, Laaziz I, Jariri S, Amrani M, Elmidaoui A. Economical evaluation of the fluoride removal by nanofiltration. *Desalination.* 2009;249:154–157.
7. Ji Y, An Q, Zhao Q, Chen H, Qian J, Gao C. Fabrication and performance of a new type of charged nanofiltration membrane based on polyelectrolyte complex. *J Membr Sci*. 2010;357:80–89.
8. Lau WJ, Ismail AF. Polymeric nanofiltration membranes for textile dye wastewater treatment: Preparation, performance evaluation, transport modelling, and fouling control-a review. *Desalination.* 2009;245:321–348.
9. Decher G, Hong J, Schmitt J. Buildup of ultrathin multilayer films by a self-assembly process: III. Consecutively alternating adsorption of anionic and cationic polyelectrolytes on charged surfaces. *Thin Solid Films.* 1992;210–211:831–835.
10. Decher G. Fuzzy nanoassemblies: Toward layered polymeric multicomposites. *Science*. 1997;277:1232–1237.
11. Krasemann L, Toutianoush A, Tieke B. Self-assembled polyelectrolyte multilayer membranes with highly improved pervaporation separation of ethanol/water mixtures. *J Membr Sci*. 2001;181:221–228.
12. Toutianoush A, Tieke B. Pervaporation separation of alcohol/water mixtures using self-assembled polyelectrolyte multilayer membranes of high charge density. *Mater Sci Eng*. 2002; 22:459–463.
13. Yoshida W, Cohen Y. Ceramic-supported polymer membranes for pervaporation of binary organic/organic mixtures. *J Membr Sci*. 2003;213:145–157.
14. Shao P, Huang R. Polymeric membrane pervaporation. *J Membr Sci*. 2007;287:162–179.
15. Ackern F, Krasemann L, Tieke B. Ultrathin membranes for gas separation and pervaporation prepared upon electrostatic self-assembly of polyelectrolytes. *Thin Solid Films*. 1998;327–329:762–766.
16. Hong S, Ouyang L, Bruening M. Recovery of phosphate using multilayer polyelectrolyte nanofiltration membranes. *J Membr Sci*. 2009;327:2–5.
17. Hong S, Bruening M. Separation of amino acid mixtures using multilayer polyelectrolyte nanofiltration membranes. *J Membr Sci*. 2006;280:1–5.
18. Jin W, Toutianoush A, Tieke B. Use of polyelectrolyte layer-by-layer assemblies as nanofiltration and reverse osmosis membranes. *Langmuir*. 2003;19:2550–2553.
19. Saren Q, Qiu C, Zhao Y, Tang C. Double-skinned forward osmosis membranes based on layer-by-layer assembly-FO performance and fouling behavior. *J Membr Sci*. 2012;405–406:20–29.
20. Saren Q, Qiu C, Tang C. Synthesis and characterization of novel forward osmosis membranes based on layer-by-layer assembly. *Environ Sci Technol*. 2011;45:5201–5208.
21. Sansiviero M, Santos D, Job A, Aroca R. Layer by layer TiO_2 thin films and photodegradation of Congo red. *J Photochem Photobiol A* 2011;220:20–24.
22. Yilmaztürk S, Ercan N, Deligöz H. Influence of LbL surface modification on oxygen cross-over in self-assembled thin composite membranes. *Appl Surf Sci*. 2012;258:3139–3146.
23. Zhang G, Gao X, Ji S, Liu Z. Electric field-enhanced assembly of polyelectrolyte composite membranes. *J Membr Sci*. 2008;307:151–155.
24. Dubas ST, Schlenoff JB. Polyelectrolyte multilayers containing a weak polyacid: Construction and deconstruction. *Macromolecules*. 2001;34:3736–3740.
25. Burke SE, Barrett CJ. Acid base equilibria of weak polyelectrolytes in multilayer thin films. *Langmuir*. 2003;19:3297–3303.
26. Buck M, Zhang J, Lynn D. Layer-by-Layer assembly of reactive ultrathin films mediated by click-type reactions of poly(2-alkenyl azlactone)s. *Adv Mater*. 2007;19:3951–3955.
27. Such G, Quinn J, Quinn A, Tjipto E, Caruso F. Assembly of ultrathin polymer multilayer films by click chemistry. *J Amer Chem Soc*. 2006;128:9318–9319.
28. Zhang G, Dai L, Ji S. Dynamic pressure-driven covalent assembly of inner skin hollow fiber multilayer membrane. *AIChE J*. 2011;57:2746–2754.
29. Jou J, Yoshida W, Cohen Y. A novel ceramic-supported polymer membrane for pervaporation of dilute volatile organic compounds. *J Membr Sci*. 1999;162:269–284.
30. Chen Y, Xiangli F, Jin W, Xu N. Organic–inorganic composite pervaporation membranes prepared by self-assembly of polyelectrolyte multilayers on macroporous ceramic supports. *J Membr Sci*. 2007;302:78–86.
31. Wang N, Zhang G, Ji S, Fan Y. Dynamic layer-by-layer self-assembly of organic–inorganic composite hollow fiber membranes. *AIChE J*. 2012;58:3176–3182.
32. Silva V, Prádanos P, Palacio L, Calvo J, Hernández A. Relevance of hindrance factors and hydrodynamic pressure gradient in the modelization of the transport of neutral solutes across nanofiltration membranes. *Chem Eng J*. 2009;149:78–86.
33. Smid J, Avci C, Gunay V, Terpstra R. Preparation and characterization of microporous ceramic hollow fibre membranes. *J Membr Sci*. 1996;112:85–90.
34. Li J, Wang L, Hao Y, Liu X, Sun X. Preparation and characterization of Al_2O_3 hollow fiber membranes. *J Membr Sci*. 2005; 256:1–6.
35. Tan X, Liu S, Li K. Preparation and characterization of inorganic hollow fiber membranes. *J Membr Sci*. 2001;188:87–95.
36. Ogunbiyi O, Miles N, Hilal N. The effects of performance and cleaning cycles of new tubular ceramic microfiltration membrane fouled with a model yeast suspension. *Desalination*. 2008;220:273–289.
37. Ismail A, Kusworo T, Mustafa A. Enhanced gas permeation performance of polyethersulfone mixed matrix hollow fiber membranes using novel dynasylan ameo silane agent. *J Membr Sci*. 2008; 319:306–312.
38. Kim D, Park H, Rhim J, Lee Y. Proton conductivity and methanol transport behavior of cross-linked PVA/PAA/silica hybrid membranes. *Solid State Ionics*. 2005;176:117–126.
39. Zhang G, Gu W, Ji S, Liu Z, Peng Y, Wang Z. Preparation of polyelectrolyte multilayer membranes by dynamic layer-by-layer process

for pervaporation separation of alcohol/water mixtures. *J. Membr. Sci.* 2006;280:727–733.
40. Zhang G, Song X, Ji S, Wang N, Liu Z. Self-assembly of inner skin hollow fiber polyelectrolyte multilayer membranes by a dynamic negative pressure layer-by-layer technique. *J Membr Sci.* 2008;325:109–116.
41. Majewska-Nowak K. Application of ceramic membranes for the separation of dye particles. *Desalination.* 2010;254:185–191.
42. Yu S, Chen Z, Cheng Q, Lü Z, Liu M, Gao C. Application of thin-film composite hollow fiber membrane to submerged nanofiltration of anionic dye aqueous solutions. *Sep Purif Technol.* 2012;88:121–129.
43. Yu S, Liu M, Ma M, Qi M, Lü Z, Gao C. Impacts of membrane properties on reactive dye removal from dye/salt mixtures by asymmetric cellulose acetate and composite polyamide nanofiltration membranes. *J Membr Sci.* 2010;350:83–91.
44. Mo Y, Chen J, Xue W, Huang X. Chemical cleaning of nanofiltration membrane filtrating the effluent from a membrane bioreactor. *Sep Purif Technol.* 2010;75:407–414.
45. Sohrabi M, Madaeni S, Khosravi M, Ghaedi A. Chemical cleaning of reverse osmosis and nanofiltration membranes fouled by licorice aqueous solutions. *Desalination* 2011;267:93–100.
46. Yoshizawa T, Shin-ya Y, Hong K, Kajiuchi T. pH— and temperature-sensitive permeation through polyelectrolyte complex films composed of chitosan and polyalkyleneoxide-maleic acid copolymer. *J Membr Sci.* 2004;241:347–354.
47. Burke S, Barrett C. Acid base equilibria of weak polyelectrolytes in multilayer thin films. *Langmuir.* 2003;19:3297–3303.

Manuscript received Aug. 26, 2012, and revision received Feb. 8, 2013.